Supporting Information

for

# Interfacial vibrational dynamics of Ice $I_h$ and liquid water

Authors:

Prerna Sudera [1], Jenée D. Cyran [1,3], Malte Deiseroth [1], Ellen H. G. Backus [1,2],*, and Mischa Bonn [1],*


Affiliations:

[1] Max Planck Institute for Polymer Research, Mainz, Germany

[2] University of Vienna, Vienna, Austria

[3] Baylor University, Waco, TX, USA

# Additional Data

Ratio of SFG spectra for ice and water at $\nu_{exc}$ = 3050 and 3310 cm$^{-1}$.



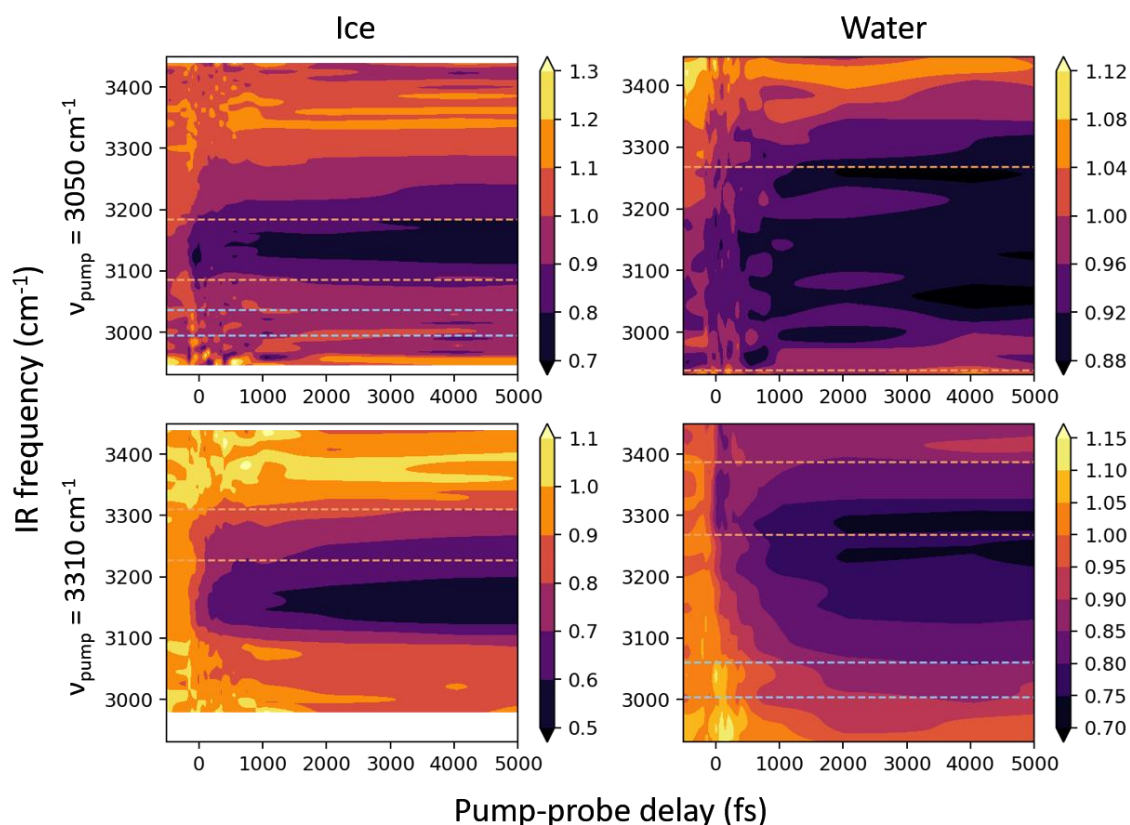Figure S1: Ratio of SFG spectra for ice and water, each excited at $\nu_{exc}$=3050 and 3310 cm$^{-1}$. Orange and sky blue dashed lines represent the spectral region integrated for the ground state bleach (GSB) and the excited state (ES) traces, respectively. Ice is measured at 248 K, and water at 278 K. Although measured at different temperatures, the data can still be compared as it is known from literature[1] that the liquid water dynamics do not significantly depend on temperature, at least from 278 to 300 K. Please note the different z-scale for the different panels. The fine structure for water pumped at 3050 cm$^{-1}$ is caused by noise, resulting from low signal levels. Boxed areas indicate integrated regions used to compile Figure S2. The specific integration intervals were chosen based on the spectral observations - see text below. By varying the integration limits, we confirmed that the results are independent of the precise value.

Figure S1 shows the ratio SFG spectra for all 4 cases – ice in column 1, water in column 2, excitation frequency = 3050 cm$^{-1}$ represented in row 1, and excitation frequency = 3310 cm$^{-1}$ in row 2. Ground state bleach is represented by ratio <1 signal; and ratio >1 signal around the low-frequency region may represent the excited state (ES) signal. Accordingly, ES SFG signal for ice with $\nu_{exc}$=3050 and water with $\nu_{exc}$=3310 cm$^{-1}$ was shown in the main text. For the other two cases, there is no clear spectral signature for the ES response observed in Fig. 1, most probably due to overlap with bleach and heat signals. The traces in Fig. S2 show this in more detail. In red are the traces shown for integrated close to the excitation frequency; in blue, the traces integrated where the excited state would be expected based on the anharmonicity. These latter traces, in principle, follow the same dynamics as the GSB (in red),

and hence are dominated mostly by bleach and heat effects. Also, the central frequency shift for the two cases, did not give elaborative information, and is shown in figure S3.

To obtain the traces in figure 2 and figure S2, specific spectral integration limits have to be set. Choosing individual integration regions for each sample and excitation wavelength is inevitable, due to a) different IR absorption line-shapes and peaking frequencies for ice and water; b) sample-dependent response for the same excitation frequency – maximum bleach being centered at different frequencies for ice and water; c) super-fast spectral diffusion, complicating the designated area of integration further to procure vibrational lifetimes.

The integration regions were hence individually defined for the two samples, reflecting their respective response to the pump excitation. More generally, ground state bleach regions were chosen to be close to the excitation frequency, incorporating spectral diffusion (movement of bleach signal at early times across spectral range), and also spectral area with high bleach signal.
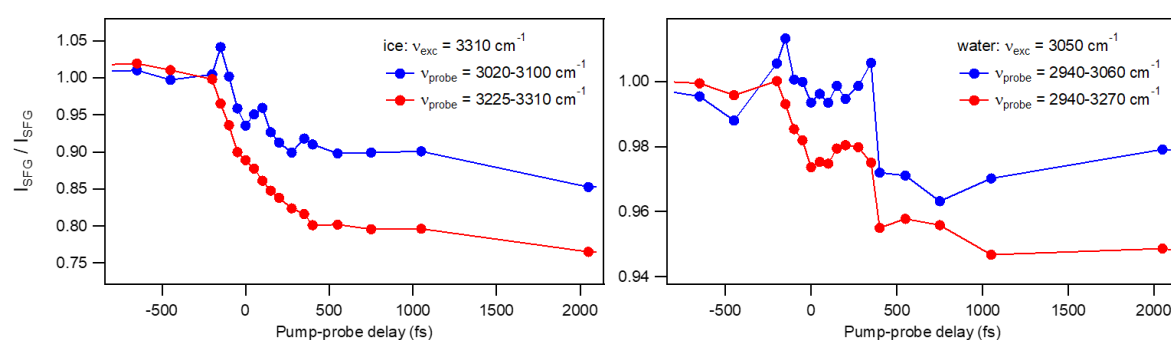


Figure S2: Integrated signal in the anharmonic frequency-shifted region for ice with $\nu_{exc}$=3310 cm$^{-1}$ and water with $\nu_{exc}$=3050 cm$^{-1}$.
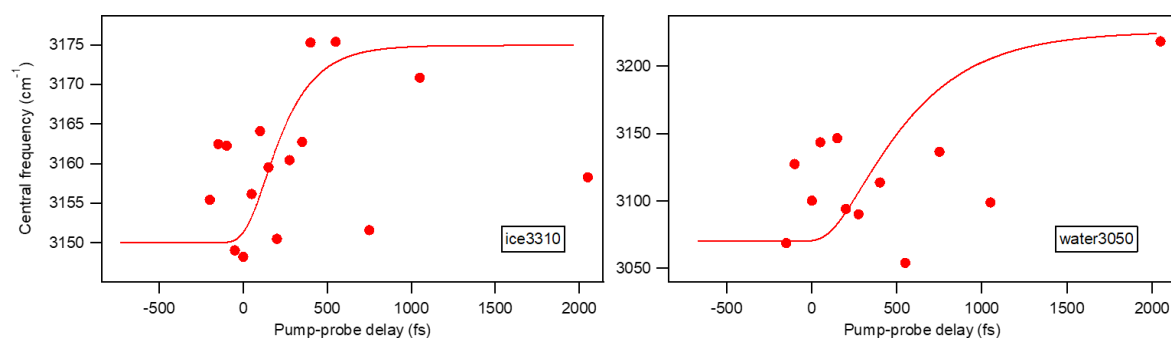


Figure S3: Central frequency as a function of pump-probe delay for ice with $\nu_{exc}$=3310 cm$^{-1}$ and water with $\nu_{exc}$=3050 cm$^{-1}$.

## Blue- vs. red-shifting of spectra

As shown in the main text, upon pumping ice at 3050 cm$^{-1}$, the first spectral moment of $I_{SFG}^{exc}/I_{SFG}^{ref}$ shifts to higher frequency upon relaxation, while it shifts to lower frequency for pumping water at 3310 cm$^{-1}$. In both cases, the shifts in the OH stretch frequencies are the result of ultrafast heating, following vibrational relaxation; that the direction of the shift is opposite is the result of the spectral position of the excitation pulse below (exciting ice at 3050 cm$^{-1}$) and above (exciting water at 3300 cm$^{-1}$) the peak of the $I_{SFG}^{exc}/I_{SFG}^{ref}$ SFG response (respectively, 3150 and 3250). Hence, for ice pumped at low frequencies,

the excitation occurs below the main response, and there is an up-shift due to the heating, while for water, there is a down-shift.

## Model

The 4-level model used to fit traces is described in the main text (see Ref [2] for details). Below are the equations used to describe the ground state bleach (GSB$_{SFG}$), excited-state SFG response (ES$_{SFG}$), and the thermal effects (Heat$_{SFG}$). $a$ and $c$ are constants scaling the contribution of the heat. $b$ is a normalization constant accounting for the difference in cross-section between the 0-1 and the 1-2 transition. As discussed in the main text, the observed frequency shift is used as a signature of the heated ground state. To model this frequency shift, we scaled and shifted the trace observed in the model by the constant $d$ and an offset.

$$GSB_{SFG}(t) = \frac{(N_0(t) - N_1(t) + N_*(t) + aN_{0*}(t))^2}{N_0(0)^2}$$

$$ES_{SFG}(t) = (1 + bN_1(t) + cN_{0*}(t))^2$$

$$Heat_{SFG}(t) = \frac{dN_{0*}(t)^2}{N_0(0)^2} + offset$$

## Methods:

1. **Ice sample preparation:**

   Single-crystalline ice was prepared using the Czochralski process. An ice seed (4 X 2cm), procured from undisturbed freezing of milliQ water, is melt-attached to a cold finger maintained at ~-15° C. A heat gun is used to create a molten water layer at the bottom surface of the attached ice seed before being dipped into clean milliQ water maintained at 0.5° C. The ice seed is only half-submerged in water; the water bath is constantly stirred, to provide dynamic energy to the water molecules to potentially stick and unstick (if in a bad position) to the seed, forming new ice. The cold finger, along with the new ice boule formed over time, is pulled out of the water bath at an optimized rate. Normally an ice boule 10 cm in diameter and thickness is obtained in ~24 hours.

   The single-crystallinity of the ice boule thus obtained is checked using a cross-polarizer setup, making use of the small birefringence of ice. All samples were oriented to the basal plane of hexagonal ice for consistency purposes. Samples from the boule were treated with Formvar, and observed under a microscope, leaving etch pits upon evaporation; the respective shape corresponds to the orientation plane of the sample. Further corrections in the orientation plane are made by sawing the ice boule after an estimation of the angles from the etch-pit shadows. Samples oriented via the etch-pit technique were checked with X-ray crystallography and were found to have an error of ~1-2° [3].

A 5mm thick, 4.4cm diameter circular sample is cut from the basal-oriented single-crystalline ice boule, and attached onto an Aluminium pin in a custom-made sample cell. The sample cell is then mounted on a microtome setup, and using a 3-faceted microtome blade, the ice surface is shaved smoothly to have an optically-flat, even surface. The cell is later closed by a $CaF_2$ window and the ice is allowed to anneal overnight at -20°C to attain a certain equilibration before measurements.

During measurement, a rotating motor-operated using a crankshaft mechanism rotates the cell on a copper stage accompanied by a wobbling motion for more surface area; so every laser pulse hits a fresh spot on the ice surface, avoiding accumulated heat effects. The copper stage is cooled down using a silicon-oil-based pump, and the ice surface can reach temperatures as low as 223 K.

2. **Laser set up:**

A 1-kHz Titanium-Sapphire regenerative amplifier (Spectra Physics Spitfire Pro) produced 800 nm, 40 fs pulses, approximately 5 mJ in energy. Part of it goes through a commercial OPA (TOPAS-c) to generate infrared pulses tunable in frequency from a range of 2800 to 3700 $cm^{-1}$, producing 3-11 μJ pulses, depending on the chosen frequency region, and 300 $cm^{-1}$ FWHM in spectral bandwidth. Another part goes through a second TOPAS, the idler output of which is sent through a BBO crystal producing doubled idler around 1075 nm center wavelength. This passes through a KTP crystal where it is overlapped by another part of the 800 nm beam to generate the IR pump, centered around 3200 $cm^{-1}$ and 100 $cm^{-1}$ in bandwidth. The remaining visible beam passes through an etalon to generate a narrow-band visible laser pulse, approximately 25 $cm^{-1}$ in spectral width, centered at 800 nm. The pump beam goes through a delay stage to change the relative timing between the Vis-IR SFG probe pair and the IR-Pump. The Visible, pump IR, and probe IR pulses hit the sample with approximately 5, 10 and 2 μJ energy, at angles of 60, 50, and 35° to the surface normal, respectively. The SFG signal was focused onto a spectrograph (Acton SP-300i, Princeton Instruments) and detected on a CCD camera (Newton 971 Andor). The SFG signal is collected in P-SSP polarization (P-polarized IR Pump; S-polarized SFG; S-polarized Visible; S-polarized IR Probe). Using a mechanical chopper, the 1kHz IR pump is chopped down to 500 Hz. The pump, along with the IR-VIS probe pair, hits the sample, and the signals in the presence and absence of the pump are detected on different regions of a charged-coupled device camera, spatially separated by a galvanometer mirror synchronized with the chopper.

# References

1. Woutersen, S., Emmerichs, U., Nienhuys, H. K. & Bakker, H. J. Anomalous temperature dependence of vibrational lifetimes in water and ice. *Phys. Rev. Lett.* **81**, 1106–1109 (1998).

2. Deiseroth, M., Bonn, M. & Backus, E. H. G. Electrolytes Change the Interfacial Water Structure but Not the Vibrational Dynamics. *J. Phys. Chem. B* **123**, 8610–8616 (2019).

3. Sánchez, M. A. *et al.* Experimental and theoretical evidence for bilayer-by-bilayer surface melting of crystalline ice. *Proc. Natl. Acad. Sci.* **114**, 227–232 (2017).